

**Supplementary Information for**

**A metasurface-based diamond frequency converter using**

**plasmonic nanogap resonators**

*Qixin Shen<sup>1</sup>, Amirhassan Shams-Ansari<sup>2</sup>, Andrew M. Boyce<sup>3</sup>, Nathaniel C. Wilson<sup>1</sup>, Tao Cai<sup>3</sup>,  
Marko Loncar<sup>2</sup>, Maiken H. Mikkelsen<sup>3,\*</sup>*

<sup>1</sup>Department of Physics, Duke University, Durham, NC 27708, USA

<sup>2</sup>John A. Paulson School of Engineering and Applied Sciences, Harvard University, Cambridge, Massachusetts 02138, USA

<sup>3</sup>Department of Electrical and Computer Engineering, Duke University, Durham, NC 27708, USA

\*Correspondence to: m.mikkelsen@duke.edu, +1 (919) 660-0185

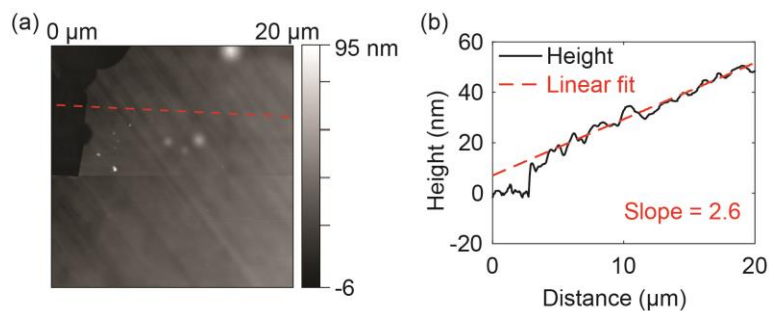
## **Fabrication method**

The samples used in this work consist of a gold ground plane on a silicon substrate, an etched diamond slab and gold nanoparticles. The 75 nm gold film was deposited by electron-beam evaporation with a 2 Å/s deposition rate. The etched diamond slab was fabricated on a 1 x 1 mm, 30 µm thick electronic-grade, single-crystal diamond thin film (Element Six). It was then mounted and etched on a sapphire carrier wafer to a submicron thickness using deep reactive-ion etching (RIE) with alternating ArCl<sub>2</sub> and O<sub>2</sub> chemistries. The thickness gradient in the etched diamond slab occurs due to the mechanical polishing process on the surface prior to etching. Once etching is complete, the slab is dewetted from the carrier wafer using a droplet of hydrofluoric acid (HF). Once the diamond is detached, the HF is diluted with DI water and the thin film is transferred and bonded onto the gold film via Van der Waals forces.

The gold nanoparticles were fabricated by electron-beam lithography (EBL) and transferred onto diamond using polydimethylsiloxane (PDMS). The nanoparticles were first fabricated on a silicon substrate. Then, a PDMS stamp was placed on top and the sample was baked at 100°C for 30 minutes. Potassium hydroxide (KOH) solution was used to etch the thin silicon dioxide (SiO<sub>2</sub>) layer on the silicon substrate for 2 hours. This results in the gold nanoparticles debonding from the silicon substrate and attaching to the PDMS stamp, which was then placed on a glass slide and stored in vacuum to dry overnight. Lastly, with the gold nanoparticles face-down, the PDMS stamp was pressed onto the diamond slab and baked at 120°C for 4 minutes. The sample was placed in vacuum for two days and then baked at 120°C for 4 minutes before removing the stamp.

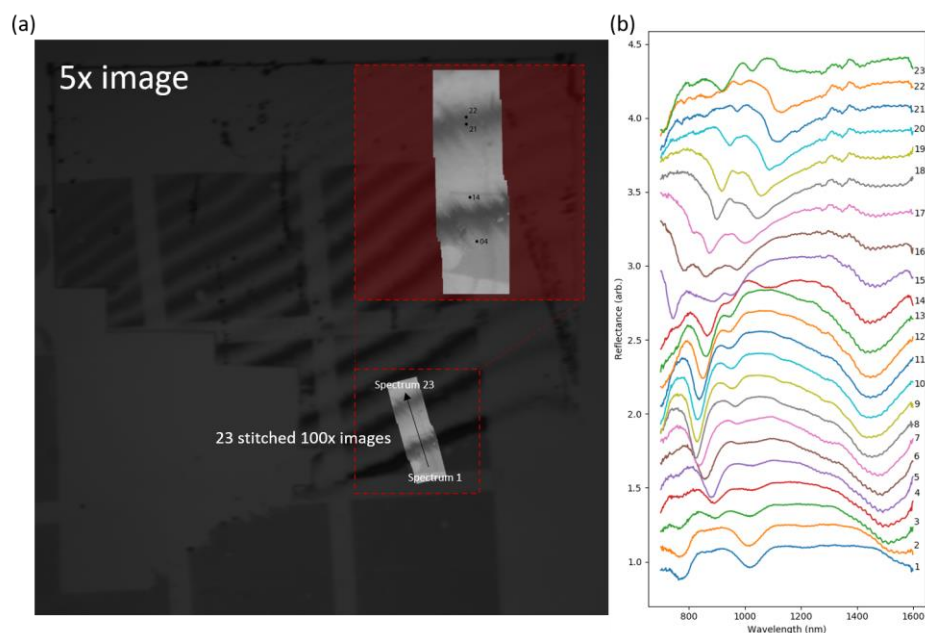
### Additional AFM characterization of the diamond slab

The diamond slab was measured by atomic force microscope (AFM) showing a 2.6 nm/ $\mu\text{m}$  gradient.



**Supplementary Figure 1:** (a) AFM image of the diamond slab. (b) Height profile along the dashed line in (a).

### Additional optical characterization of the diamond slab



**Supplementary Figure 2:** (a) Optical image of diamond slab with inset areas of measured reflection spectra. (b) Measured reflection spectra from the area indicated in (a) for increasing thickness of diamond, normalized to gold.

## **Optical setup**

### *Nonlinear response measurements*

The samples were excited using a Ti:sapphire laser (Coherent Chameleon, ~150 fs pulse duration, 80 MHz repetition rate) and an optical parametric oscillator pumped by the same Ti:sapphire laser. A beam splitter is used to overlap the two laser pulses spatially and a variable delay line allows for control over the relative time difference between the two laser pulses. Then the two excitation pulses were focused onto the sample plane using a microscope objective lens (Mitutoyo M Plan Apo NIR, 100×). The same objective was used to collect the nonlinear response in a reflection geometry, and the signal was passed through a dichroic mirror (650 nm longpass) along with two short-pass filters (600 nm and 650 nm cutoff) before being detected by a CCD camera (Princeton Instruments 400 BR Excelon) attached to a spectrometer (Acton sp2500i). The dichroic mirror was changed to an 800 nm longpass and the short-pass filters were changed to 785 nm and 1000 nm cutoff wavelengths when measuring second harmonic generation (SHG) response.

### *Reflection measurements*

The 700 nm – 1000 nm spectral range was measured using a charge-coupled device (CCD) camera and 1000 nm – 1700 nm spectral range was measured with an indium-gallium-arsenide (InGaAs) camera.

### *Determining nonlinear generation efficiency*

A calibrated light source (Labsphere) is positioned at the focal plane of the objective lens and the photon counts are collected by the CCD camera-coupled spectrometer (same as used for the nonlinear response measurements). From this, a linear relation between radiative power and detected photon counts are obtained. The nonlinear generation power is converted from the

nonlinear response counts using this relation and the efficiency is determined as the nonlinear generation power divided by the excitation power.

### **Nonlinear response enhancement factor**

The enhancement factor is defined as the nonlinear intensity from the plasmonic structures divided by the intensity from bare diamond on PDMS under the same excitation conditions. Note that different excitation powers are used to generate the nonlinear response in order to prevent damage to the nanocavities due to heating from the localized electric field. In light of this, the nonlinear intensities are extrapolated to the same excitation power using the confirmed power law that was also used to derive the enhancement factor.

### **Efficiency comparison between this work and previous literatures**

Table S1. Efficiency comparison between this work and previous literatures		
	THG	SHG
This work	$2.33 \times 10^{-5} \%$	$7.59 \times 10^{-6} \%$
Opt. Express 20, 4856 (2012)	NA	$1.4 \times 10^{-6} \%$
Nano Lett. 11, 5519 (2011)	NA	$1.8 \times 10^{-7} \%$
Nat. Nanotechnol. 10, 412 (2015)	NA	$6.4 \times 10^{-7} \%$
Nat. Nanotechnol. 9, 290 (2014)	$7 \times 10^{-4} \%$	NA
Opt. Express 26, 20718 (2018)	$5.06 \times 10^{-7} \%$ - $8.78 \times 10^{-4} \%$	NA
ACS Photonics 7, 901 (2020)	$7.44 \times 10^{-4} \%$	NA

## Coupled mode theory analysis of nonlinear responses

The dependence of the nonlinear intensity on the excitation power  $P_{1(2)}$  and the excitation frequency detuning  $\Delta\omega_{1(2)}$  from the respective resonant frequencies are analyzed by coupled mode theory:

$$\begin{aligned}
 P^{SHG} &\propto P_1^2 \left[ \frac{\gamma_{r1}}{\gamma_1^2 + \Delta\omega_1^2} \right]^2 \\
 P^{SFG} &\propto P_1 P_2 \left[ \frac{\gamma_{r1}}{\gamma_1^2 + \Delta\omega_1^2} \right] \left[ \frac{\gamma_{r2}}{\gamma_2^2 + \Delta\omega_2^2} \right] \\
 P^{THG} &\propto P_1^3 \left[ \frac{\gamma_{r1}}{\gamma_1^2 + \Delta\omega_1^2} \right]^3 \\
 P^{FWM} &\propto P_1^2 P_2 \left[ \frac{\gamma_{r1}}{\gamma_1^2 + \Delta\omega_1^2} \right]^2 \left[ \frac{\gamma_{r2}}{\gamma_2^2 + \Delta\omega_2^2} \right]
 \end{aligned} \tag{1}$$

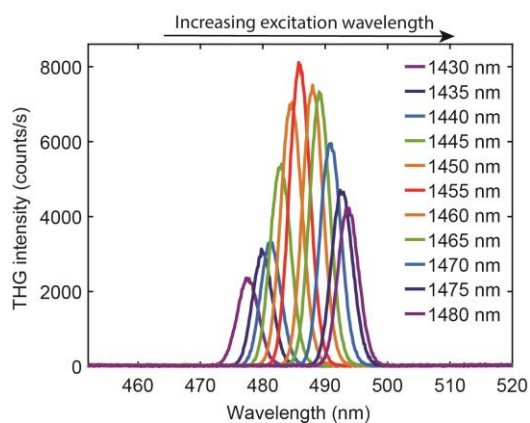
where we assumed that there is a predominant mode around the resonance frequency,  $\omega_{1(2)}$ , and  $\gamma_{i(ri)}$  denotes the total (radiative) decay rate of the mode at  $\omega_i$ . Therefore, the dependence of the nonlinear intensity on the excitation frequency detuning  $\Delta\omega_{1(2)}$  can exhibit a higher-order Lorentzian response.

## The full-widths at half-maximum (FWHM) of the THG and SHG enhancement as a function of excitation wavelength

The FWHM of THG and SHG enhancement as a function of excitation wavelength is derived by fitting the experimental results with a Lorentzian function. It is observed that these FWHMs from nonlinear response is much smaller than the FWHM of the cavity's reflection spectrum. The ratio between the FWHM of THG enhancement (31 nm) and the FWHM of

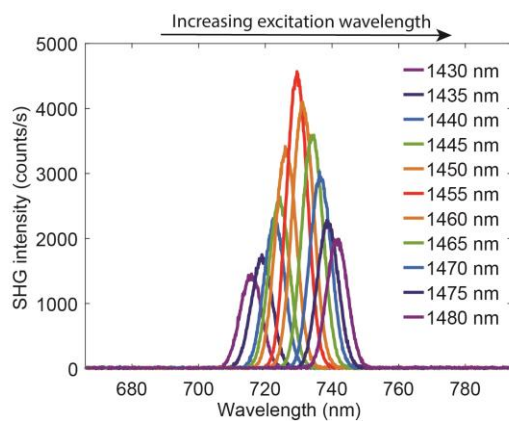
reflection spectrum (204 nm) is 0.15 in experiment, while the ratio is quantitatively expected to be  $\sqrt{\sqrt[3]{2}-1}$  (0.51) due to the 3<sup>rd</sup> order Lorentzian lineshape of THG compared with the simple Lorentzian lineshape of the reflection spectrum. The discrepancy is likely due to the relatively low quality factor of the plasmonic gap mode, as the coupled mode theory analysis assumes that mode amplification only occurs at the resonant frequency with an infinitely large quality factor. Similarly, the ratio between the FWHM of SHG enhancement (40 nm) and the FWHM of reflection spectrum (204 nm) is 0.20 in experiment, while the ratio is quantitatively expected to be  $\sqrt{\sqrt{2}-1}$  (0.64) due to the 2<sup>nd</sup> order Lorentzian lineshape for SHG. Qualitative agreement between experiment and theory is achieved for both THG and SHG in terms of the narrowed bandwidth of excitation wavelength dependent nonlinear response compared with the cavity reflection spectrum. On the other hand, the ratio between the FWHM of THG enhancement and the FWHM of SHG enhancement agrees well as the experimental ratio is  $\frac{31}{40} = 0.78$  and ratio derived from coupled mode theory analysis is  $\frac{\sqrt{\sqrt[3]{2}-1}}{\sqrt{\sqrt{2}-1}} = 0.79$ . This good agreement is likely a result of the effect of the quality factor occurring for both THG and SHG, thus compensating for each other.

### Additional experimental data of THG intensity as a function of excitation wavelength



**Supplementary Figure 3:** THG response spectra as a function of excitation wavelength.

### Additional experimental data of SHG intensity as a function of excitation wavelength



**Supplementary Figure 4:** SHG response spectra as a function of excitation wavelength.